NIOBIUM-BEARING INTERSTITIAL-FREE STEELS: PROCESSING, STRUCTURE AND PROPERTIES

Todd M. Osman [(1)] and C. Isaac Garcia [(2)]

(1) U. S. Steel Research.
(2) Basic Metals Processing, Research Institute, University of Pittsburgh.

Abstract

The relationships between metallurgy and the production of niobium-bearing interstitial-free steels are reviewed. Processing-structure-property relationships are discussed, beginning with modern steelmaking processes and continuing through subsequent thermomechanical processing. Interstitial-free stabilization, microstructural development, and mechanical properties of niobium-bearing interstitial-free steels are reviewed as well as the influence of niobium on coating characteristics.

Introduction

Interstitial atoms, such as carbon and nitrogen, have a marked effect on the deformation behavior of steel. Discontinuous yielding in steel is strongly related to interstitial species (1, 2). In fact, it has been found that a yield point will persist even with an interstitial carbon content of 0.001 weight percent (10 ppm) (3). Solute carbon and nitrogen may also degrade the formability (in particular work hardening) of a steel. Furthermore, discontinuous yielding may result in Lüders bands, which are detrimental to surface appearance, and may also promote premature breakage during forming or non-uniform springback after deformation.

In order to combat the detrimental effects of interstitial species, steels have been developed which are essentially devoid of solute carbon and nitrogen. These "interstitial-free" steels predominantly rely upon the solid state precipitation of carbides, nitrides, and carbo-sulfides to reduce the solute interstitial content. Additionally, the total carbon and nitrogen contents are reduced to extremely low levels (typically less than 0.005 weight percent carbon and less than 0.006 weight percent nitrogen) through modern steelmaking techniques.

From the earliest stages of development, it was apparent that these steels had different product attributes than traditional steel grades (4-6). Initially, these steels were produced in small quantities for laboratory studies, which focused on the deformation mechanisms of iron (4,5). This work verified that homogeneous (i.e., continuous) yielding was promoted and the formability characteristics were enhanced when compared to typical low-carbon steels.

The earliest examples of interstitial-free steels predominantly relied upon either titanium additions or niobium additions for stabilization of the interstitial species. Because of the higher cost of production, there was insufficient commercial demand to convert from traditional DQSK steels to interstitial-free steels until automobile manufacturers sought to increase corrosion resistance in the mid-1970s. With the increased utilization of hot-dip galvanized coatings, interstitial-free steels became commercially viable since these grades did not require a pre- or post-anneal to prevent strain aging.

Today, hot-dip galvanneal coated interstitial-free steels processed through continuous galvanizing lines predominantly contain a combination of titanium and niobium for interstitial-free stabilization. Additionally, some hot-dip galvanize coated sheets as well as batch annealed sheets (i.e., cold rolled or electrogalvanized sheets) contain titanium and niobium, especially higher tensile strength grades. The remaining interstitial-free steels currently produced rely upon titanium additions alone for interstitial stabilization.

In light of the commercial importance of interstitial-free steels, in particular for hot-dip galvanneal coating, the following sections seek to summarize many of the metallurgical features that control the interstitial content. In particular, the processing-structure-property relationships for titanium-niobium (TiNb)-stabilized interstitial-free steels for hot-dip galvanneal coating will be discussed.

Control of Interstitial Content

The control of interstitial-free content in interstitial-free-steels can be divided into two main subject areas: i) steelmaking and casting and ii) precipitation. The main goal in steelmaking and casting is to limit the total content of carbon and nitrogen while precipitation ensures the removal of solute interstitial-free atoms in the final product.

A significant reduction in the carbon content of liquid steel occurs during oxygen steelmaking (7-9). Whether top blown (BOP*) or bottom blown (Q-BOP) technologies are utilized, carbon is removed from the melt via gaseous carbon monoxide or carbon dioxide.

Figure 1 illustrates the change in carbon content that occurs through oxygen steelmaking. Oxygen introduced to the liquid steel through Q-BOP tuyeres begins, for example, to react with carbon after the depletion of silicon. The rate at which carbon is removed is related to the supply of oxygen to the hot metal and is approximately linear with time until late in the process (approximately 0.3 weight percent carbon in Figure 1). Past this point, further removal of carbon is controlled by the mass transport of carbon to a reaction interface. Typically, lower carbon contents are produced using a Q-BOP vessel due to a greater stirring intensity.

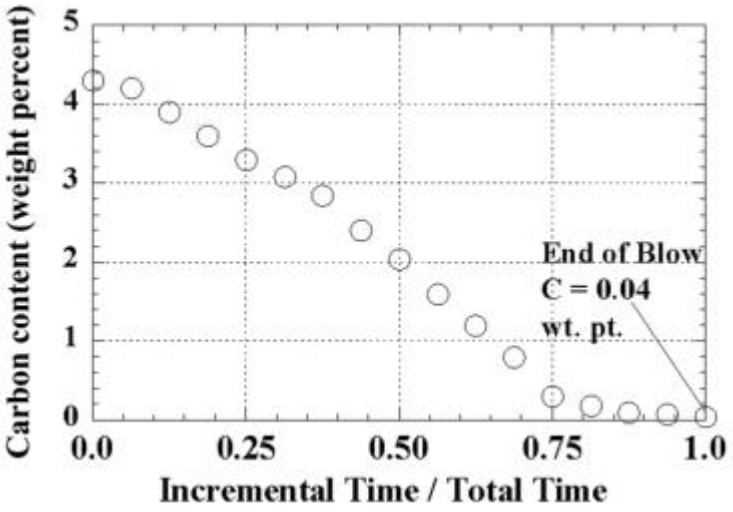

Figure 1: Change in carbon content (in weight percent) during oxygen steelmaking (BOP) (7).

After processing through a Q-BOP or BOP, the carbon content will typically range between 0.01 and 0.04 weight percent. In order to achieve the ultra-low carbon (i.e., < 0.005 weight percent) levels utilized in interstitial-free steels, the liquid metal is processed through a vacuum degasser (10-13). As shown in Figure 2, the circulation-type degasser typically utilized for interstitial-free steel production contains two snorkels (i.e., refractory tubes) that are submerged in a ladle of liquid steel. A vacuum is created in the chamber above the steel and argon is injected into the steel through one of the snorkels. The reduced density resulting from argon injection causes steel to flow into the vacuum chamber and subsequently back to the ladle via the opposite snorkel.

In this process, carbon is removed as carbon monoxide through reaction with dissolved oxygen, oxygen gas that is injected through lances or tuyeres, or iron oxide from the slag. The reduced pressures utilized during vacuum degassing favor the formation of gaseous carbon monoxide. The rate of decarburization will be related to the pressure in the vacuum chamber, the oxygen content, and the mass transport of carbon.

* Basic Oxygen Process

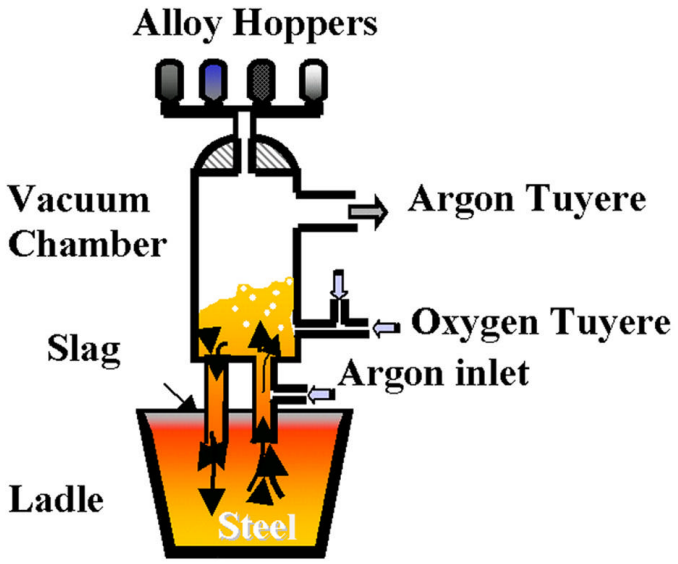

Figure 2: Illustration of a RH-type degasser.

After degassing is complete, aluminum is added to "kill" (i.e., deoxidize) the steel and the appropriate alloy additions are made, including the titanium and niobium necessary to stabilize the steel. Care must be taken, however, when processing the steel after degassing to avoid subsequent increases in carbon content. Stouvenot (13) reported an increase in carbon content of approximately 10 ppm could occur after degassing. As a result, it is important to limit the carbon content of ladle and tundish refractories, alloying additions, and any casting powders that might be utilized.

The reduction in carbon content is only part of the criteria for the steelmaking of interstitial-free steels. The nitrogen content must also be reduced to ultra-low levels, typically less than 40 ppm. The nitrogen levels are primarily reduced during oxygen steelmaking due to the stirring action of gases such as carbon monoxide. Van der Knoop, et al. (14) reported a decrease in nitrogen content from 60 ppm to less than 20 ppm through standard BOP processing. Lower nitrogen contents may be produced using a Q-BOP due to the increased intensity of gaseous stirring, especially if carbon dioxide is used in place of argon (15).

In all practicality, oxygen steelmaking is the only method to reduce the nitrogen content of liquid steel. While some decrease in soluble nitrogen could occur in vacuum degassing, long times are necessary for a significant reduction. After oxygen steelmaking, prevention of contact between the liquid steel and nitrogen bearing species, most notably air, is paramount. Nitrogen pick-up after oxygen steelmaking (i.e., after tapping the steel from the BOP/Q-BOP furnace through the caster mold) has been reported to be between 4 ppm and 30 ppm (14, 15), depending on the practices utilized. As a result, the production of ultra-low nitrogen levels is favored by effective shrouding of the ladle and proper selection of tundish and mold powders.

Finally, the amount of sulfur in the steel will also affect interstitial stabilization, as detailed below. The control of sulfur content is most often accomplished in the transfer ladle prior to oxygen steelmaking (16). Typically, desulfurization reagents, such as magnesium, lime, and calcium carbide, are injected into the liquid steel. The sulfur is effectively removed from the

melt and incorporated into the slag*, while the process is enhanced through the use of long residence times of the reagent in the metal and the use of small reagent particles. If ultra-low sulfur levels are desired (i.e.., < 0.004 weight percent), further desulfurization can be performed during vacuum degassing by introducing the reagent after deoxidation of the steel. It is noted that proper care must be taken at all steps to avoid contamination of the liquid steel by sulfur-rich slags.

Interstitial Stabilization via Precipitation

The control of nitrogen, carbon, and sulfur content during steelmaking and casting is the first step in production of interstitial-free steels. The next critical metallurgical process is the removal of solute nitrogen and carbon from solution via precipitation reactions. Solute nitrogen is effectively removed from solid solution via TiN or AlN precipitation. The stabilization of carbon, however, may differ in a variety of interstitial-free steels and has been the subject of many studies (17-34). Based on the information published in the literature, several possible mechanisms for the stabilization of carbon in interstitial-free steels have emerged. In the early days of research into interstitial-free steels, it was assumed that interstitial-free steels could be considered as dilute microalloyed (HSLA) steels. That is, the precipitation behavior in these two types of steels was thought to be similar, except for the amount of precipitates formed. Based on this view, the products of the precipitation reactions were assumed to be as follows: AlN, TiN, TiS, TiC, and Nb(C,N). It is now well known that there are several types of interstitial-free steels where the precipitation behavior might be different depending on subtle differences in steel compositions (22-28).

Niobium additions are typically made to stabilize interstitial species; however, there are cases where solute niobium will be desired for property development. As will be discussed in subsequent sections, niobium additions to these grades may be made to enhance other properties. This solute niobium has been shown to segregate to grain boundaries, to subgrain boundaries, and to free surfaces. The benefits of solute niobium may be substantial. Hook et al. (39, 40) showed a strong relationship between the solute niobium level and both the final texture and formability. In addition, the segregation of niobium to the grain boundaries will become important in the microstructural development of galvanneal coatings as well as cold work embrittlement resistance, as discussed in more detail in later sections.

In these grades, interstitial stabilization primarily occurs through precipitation with titanium, similar to that found in Ti-stabilized steels. The traditionally accepted precipitation sequence in Ti-stabilized steels with atomic ratio S:C:N. 1:1:1, is TiN, TiS*, $Ti_4C_2S_2$ and TiC, as the temperature decreases. The amount of Ti required to fully stabilize interstitial-free steels was expressed as (wt%):

$$Ti_{stabilize} = 3.42N + 1.5S + 4C$$

The traditional view of stabilization is illustrated schematically in the stabilization map shown in Figure 3. This map may be applicable to microalloyed and interstitial-free steels with low S and/or high Mn. The solubility product of TiC can be described as (35):

---

* For example, when using magnesium additions, sulfur is removed from the liquid steel by the following reaction: $\underline{Mg} + \underline{S} = MgS_S$

* It is noted that both MnS and TiS have the potential to precipitate and that MnS precipitation may preferentially occur in grades with high manganese contents.

$$\text{Log } K_{sp,\,TiC} = \log \{[Ti][C]\} = 9.0 - 10330/T$$

where T is the temperature in Kelvin, [Ti] and [C] are solute concentration in weight percent. This solubility product can be used to predict the precipitation temperature in a Ti-stabilized steel. For steels whose compositions are above the stoichiometric line ($Ti^*/C = 4$, $Ti^* = Ti_{total} - 3.42N - 1.5S + Nb/1.94$), there is sufficient titanium to stabilize carbon. However, whether complete stabilization can actually be obtained is also dependent on the kinetics of the reaction. Hence, similar steels may exhibit different levels of stabilization (or different precipitates) depending upon the thermomechanical processing schedules employed in the hot strip mill.

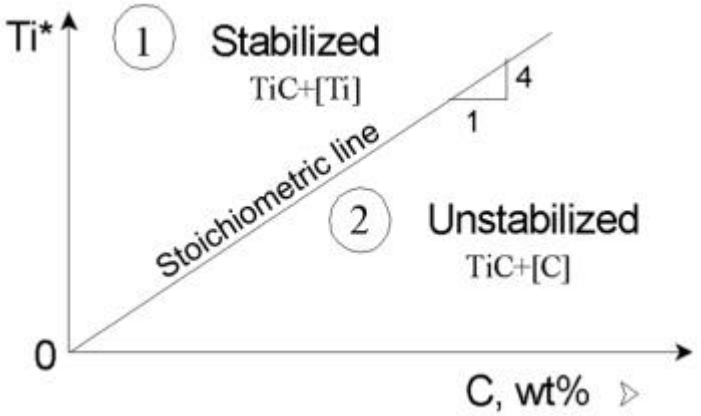

Figure 3: Traditional precipitation map. Above the stoichiometric line ($Ti^*/C = 4$, $Ti^* = Ti_{total} - 3.42N + Nb/1.94$), there is sufficient Ti and steel is generally considered as stabilized by forming TiC (36).

The early work described above did not consider the mechanism of the formation of $Ti_4C_2S_2$ or H-phase (for its hexagonal crystal structure). The work by Hua et al. (24-27) has shown that the formation of the H-phase is not by independent nucleation and growth, but rather by the in-situ transformation of TiS. This work led to a proposed stabilization map, Figure 4, for interstitial-free steels that contain 9R-TiS as major sulfides in the as-reheated condition (36).

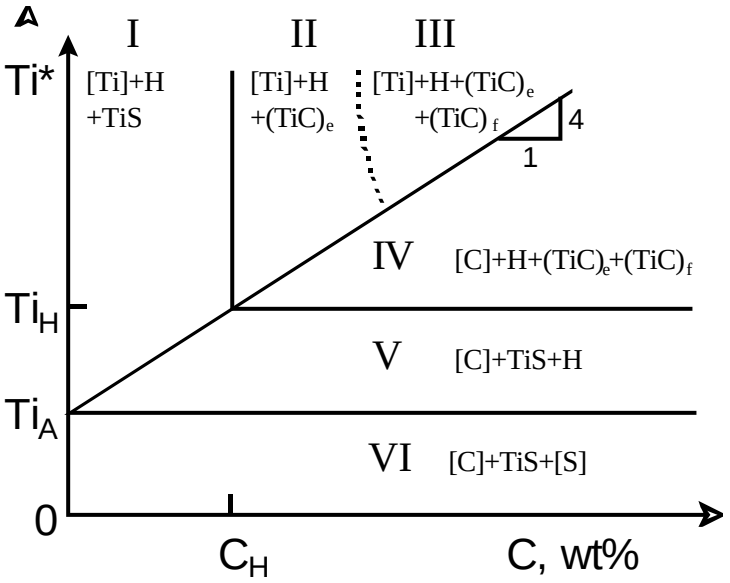

Figure 4: Proposed precipitation map for S-containing, Ti-stabilized steels ($Ti^* = Ti_{total} - 3.42N + Nb/1.94$) (36).

The above discussion describes the stabilization sequence in grades that rely solely upon titanium for stabilization. The majority of commercially produced TiNb-stabilized grades, however, will not solely rely upon titanium for interstitial stabilization. In these grades, the role of niobium as a precipitate former must also be considered. According to the traditional approach, titanium additions are made to combine with nitrogen and sulfur, while niobium additions are made to account for carbon, as shown by the following relationships:

$$Ti_{stabilize} = 3.42N + 1.5S$$
$$Nb_{stabilize} = 7.74C$$

More recent work (37) has indicated that not all of the TiS polytypes can transform directly into Ti4C2S2 or H-phase. In fact, when the dominating polytype is 6R-TiS in the as-reheated condition, the transformation of this polytype into the H carbosulfide, upon cooling, would be retarded and a hysteresis loop is observed for the reversible TiS to H transformation, Figure 5. The existence of a hysteresis loop has also been observed by Dupuis, et al. (22). The temperature dependence of the reversible R-TiS to H transformation is critical for understanding the process of carbon stabilization as it occurs during slab reheating and subsequent processing in the hot-strip mill.

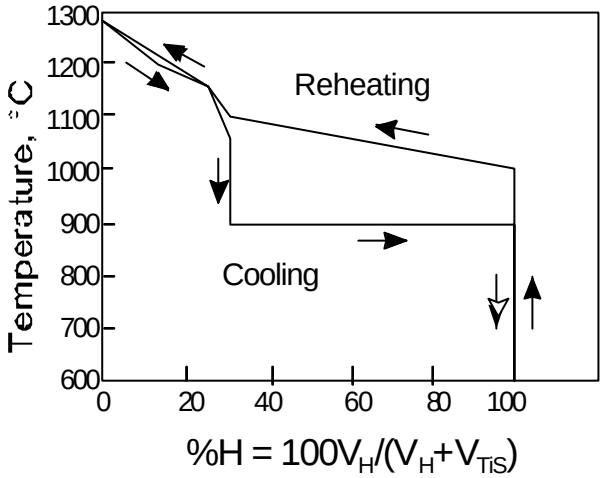

Figure 5: Hysteresis in the reheating and cooling transformation between 9R-TiS and H- Ti4C2S2 (21).

According to the traditional approach, the predominant precipitates would be TiN, TiS, $Ti_4C_2S_2$, and NbC, with the amount of each primarily depending upon composition. Recent work has shown that niobium may also be present in a complex carbo-sulfide (i.e., $(Ti, Nb)_4C_2S_2$) (20). Under these circumstances, precipitation scenarios similar to that for the Ti-stabilized grades shown in Figure 4 may be possible. As a result, depending on the alloy composition and the thermal profile during hot rolling, NbC and/or H phase may be present. It is noted that, depending upon the titanium level, a substantial amount of niobium* may remain in solid solution (24-28). In such cases, the solute niobium may be beneficial for property development, especially with respect to hot-dip galvanneal coatings.

The stabilization of interstitial species is not only sensitive to thermomechanical processing during hot rolling, but will also be influenced by the thermal cycles employed during annealing. Thermodynamically, the annealing temperature should be below the dissolution temperature for the stabilizing precipitate. TiN is stable at the annealing temperatures typically employed

* As much as 67% of the total Nb in a 0.06Ti steel.[25-27)]

during commercial annealing; however, carbide dissolution may occur, especially if NbC is the stabilizing precipitate. The amount of carbide dissolution during soaking and the degree of re-precipitation during cooling will be governed by kinetics. For the production of interstitial-free steels, care should be taken when selecting annealing cycles as to avoid carbide dissolution. Although not the subject of the current review, it is noted that carbon stabilization and carbide dissolution is an important consideration in the design of bake-hardenable steels, which require a controlled amount of solute carbon for the desired property attributes. In this case, it might be desirable to employ alloy design (i.e., be in Region II of Figure 3 or Regions IV and V in Figure 4) or to utilize annealing temperatures above the carbide dissolution temperature to produce the necessary solute carbon.

In summary, the control of interstitial species begins with steelmaking and casting techniques, which are primarily designed to minimize the amount of nitrogen and carbon in the steel. Subsequently, the stabilization of nitrogen and carbon via precipitation reactions will be determined by thermomechanical processing on the hot strip mill and during annealing.

Texture Development in Niobium Bearing Interstitial-Free Steels

As mentioned earlier, interstitial-free steels exhibit high r-values, which are beneficial for formability, especially with respect to deep drawing. The enhanced drawability is normally attributable to the existence of the gamma-fiber, ND || {111}, recrystallization texture after annealing. However, the origin of this and other texture components is still under debate. Hutchinson et al. (41) indicated that adequate control of both hot band grain size and hot band texture are fundamental to enhancing the formability properties of the final annealed material. From this observation it becomes obvious that the thermomechanical (TMP) parameters used during hot rolling affect the transformation texture and the hot band microstructure. In fact, the texture present in the ferrite structure after the material has been coiled will be strongly dependent on the texture of the austenite as it approaches the Ar_3 transformation temperature. Therefore, the transformation texture will depend on several factors, including chemical composition, TMP conditions and the microstructural state of the austenite. For example, in early work it was thought that the chemical composition of the material was the key parameter. As discussed above, carbon may be stabilized as $Ti_4C_2S_2$ (H-phase) in addition to the traditional M(CN) precipitation. Whether carbon is stabilized by the formation of either M(CN) or H depends on the overall composition of the steel, and may affect the final microstructure and texture of the hot band material. For example, it has been indicated (42, 43) that the presence of suitably dispersed Nb(CN) precipitates in the hot band material may lead to sharp {111}<uvw> annealing textures. Also, some investigators have shown that texture development in interstitial-free steels is not as susceptible to compositional and processing parameters as are AKDQ steels (44,45).

The role of alloying elements on the development of texture has also been investigated for their influence on the recrystallization behavior of austenite. For example, at high temperatures of rolling (above the austenite stop recrystallization temperature,T_{95}), a relatively weak recrystallization texture is obtained. In this case, the austenite has been determined to exhibit the cube, {100}<001>, family of orientations, which is considered to transform in ferrite into the rotated cube, {100}<011> (46). On the other hand if the austenite is unrecrystallized during hot rolling, it has been shown that a strong texture is developed in the austenite containing the brass-component, {110}<112> and copper-component, {112}<111>, which are both very stable end orientations of the beta-fiber, as well as weaker intensities of the S-component, {123}<634> and Goss-component, {110}. Upon transformation below the Ar_3 temperature, these orientations are transformed to {332}<113> (from the brass-component), {113}<110>

(from the copper-component) (48), {111}<110> (from the Goss-component) (49), respectively. In summary, solute elements that retard the recrystallization of austenite during hot rolling will have a strong effect on the transformation textures. For example, in interstitial-free steels it has been observed that niobium additions produce strong texture components near {112}<110>, together with weaker components such as {001}<110> and {332}<113>, while in Ti-stabilized steels the strongest component is {001}<110>, with weak components {112}<110> and {332}<113> (49-54). The difference in the intensity of the transformation texture products in niobium-bearing interstitial-free steels has been attributed to the suppression of the recrystallization of austenite during hot rolling through the combined effect of solute drag and precipitation (22, 40, 49-56). The effect of other solute elements (e.g., manganese, nickel, molybdenum, and chromium) on the transformation textures in steels has also been investigated.

Inagaki (57, 58) studied the effect of manganese on transformation textures with and without niobium additions. The results of these studies clearly showed that the presence of niobium increased the sharpness of the transformation textures independent of the manganese content. Inagaki suggested that the solute effect might be related to the transformation behavior by means of variant selection and/or selective growth of certain ferrite orientations during transformation (58).

The effect of TMP variables on the transformation texture and final mechanical properties of interstitial-free steels has also been well documented. Among these, the slab reheating temperature, the finishing temperature, the coiling temperature, the amount of deformation during hot and cold rolling, and the annealing temperature have been the most widely investigated (30, 60, 59-75). The slab reheating temperature, along with the type of stabilization (i.e. solubility product), controls the dissolution of precipitates, and hence, the austenite grain size. In general, low slab reheating temperatures have been shown to be beneficial in obtaining high r-values in cold rolled and annealed sheet steels. Low slab reheating temperatures seems to keep TiC and NbC precipitates from going into solution, leading to a dispersion of coarse precipitates in the hot band. The presence of coarse and widely spaced precipitates allows rapid growth of new grains, thereby helping to achieve stronger {111} textures. Another possible explanation might be due to the fact that at low slab reheating temperatures carbon may be stabilized as $Ti_4C_2S_2$ precipitates, which may lead to high r-values (60, 70). The effect of slab reheating temperature is more pronounced in Ti-stabilized steels than in TiNb-stabilized steels.

The effect of finishing temperature has also been investigated by several authors (59-61, 71-73). It is generally accepted that improvements in r-values can be achieved by lowering the finishing temperature in austenite, especially in Nb-bearing interstitial-free steels with low Nb/C ratio. Butrón-Guillén and Jonas (73) observed an increase in the gamma-fiber intensity with decreasing finishing temperature, down to 620 °C. The finishing temperature should be selected to provide uniform and fine-grain microstructure in the hot band. In the case of Ti-stabilized steels, the finishing temperature has very little effect on the r-values and ductility. The effect of the coiling temperature is important because it affects the size, distribution and morphology of precipitates. It has been observed that coarse, widely spaced precipitates enhance the development of (111) texture, which is well-known to result in high r-values, whereas fine, dense precipitates inhibit recrystallization and grain growth causing the properties to be relatively inferior (30). In general, it has been observed that increasing coiling temperature leads to higher r-values, n-values, and ductility, with a decrease in strength in Ti-stabilized steels (30, 74, 75). In Nb- and TiNb-stabilized steels, the effect of coiling temperature is more pronounced, with r-values and ductility increasing as the coiling temperature is increased (34, 42-44).

Recent work by Ruiz-Aparicio, et al. (46, 80) has suggested that the favorable gamma-fiber texture in interstitial-free steels can be obtained when large deformations are applied to coarse austenite grains. According to the authors, the major mechanism responsible is the presence of Goss nuclei within the shear bands that are generated by plastic instability. These nuclei subsequently give rise to the {111}<110> transformation texture according to the Kurdjumov-Sachs orientation relationship. The more important points from the work by Ruiz-Aparicio, et al. are:

a) The transformation texture in steels stabilized through the formation of H-phase in the interstitial-free steels is not very sensitive to processing conditions during hot deformation. The resultant crystallographic texture in the hot band for a Ti- only and Ti/Nb-stabilized steels showed similar behavior, with a strong {111}<110> hot band texture component as the main orientation in the alpha-fiber (see Figure 6). The only difference is the presence of the rotated cube orientation in this fiber for TMP in the austenite recrystallization region. The resultant intensities of {111} texture components in the gamma-fiber are similar for both steels regardless of the hot deformation schedule.

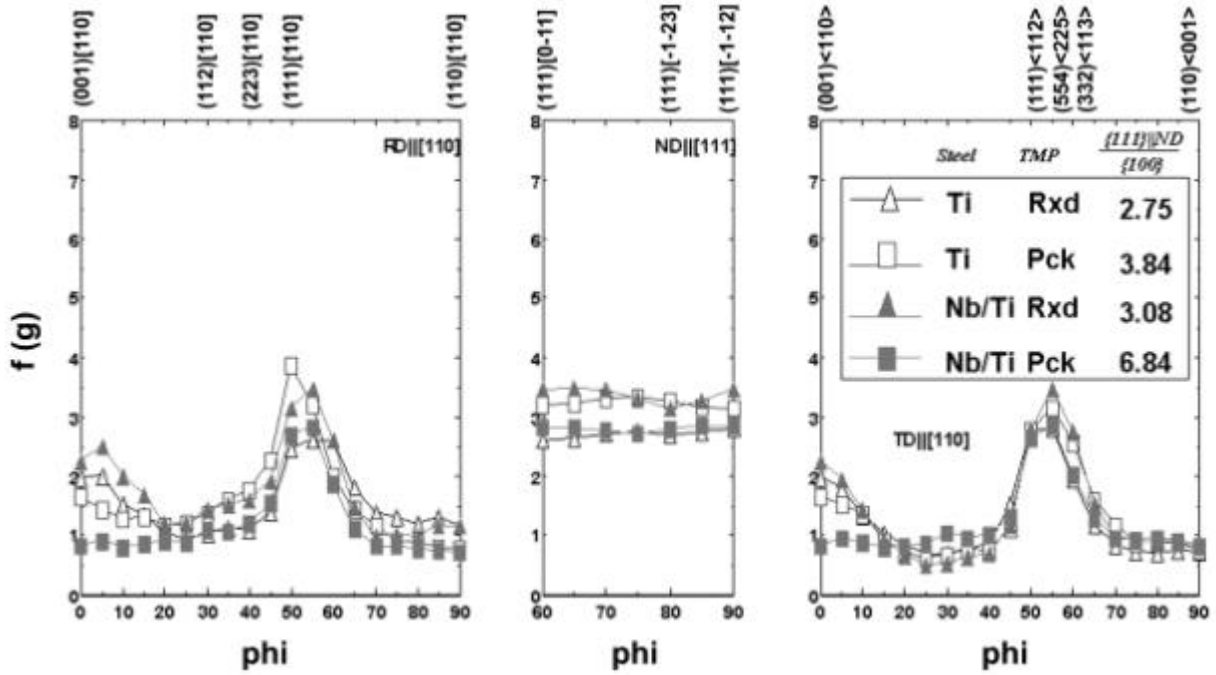

Figure 6: Texture fibers for as-coiled material (80).

b) A comparison of steels stabilized by MCN and H-phase, the H-stabilized steels showed a strong {111}<110> hot band texture component, which is the main orientation in the alpha-fiber, RD || <110>. In addition, the resultant intensities of {111} texture components in both the alpha- and gamma-fibers are higher. When the alloying elements are present in the form of strain-induced carbides or carbonitrides, there is a shift of the texture towards the rotated cube component, producing orientations varying from {113}<110> to {223}<110>.

c) Under conditions of large deformation and coarse austenitic grain sizes, the main components of the transformation textures are the gamma fiber. There seems to be an excellent correlation between the intensity of these components and the initial grain size, leading to the conclusion that coarse austenitic grain size might be responsible for the final ferritic hot band texture. Microstructural heterogeneities generated during the

heavy deformation, such as shear bands, are believed to be responsible for the observed transformation texture.

The discussion above only considers traditional hot rolling in which deformation occurs in the austenite phase field. Recently, research has been conducted involving hot strip mill rolling in the ferrite phase field (i.e., ferritic rolling). Interstitial-free steels continuously rolled in the ferrite region have been reported to exhibit higher drawability (r-values ~ 3.0) when compared to steels rolled in the austenite region. Other microstructural features and properties that have been attributed to ferritic rolling are finer grain sizes and higher yield and ultimate tensile strengths (77-79). Butrón-Guillén and Jonas (77) observed that ferritic rolling produced textures that were approximately twice as intense as those attained after rolling in the austenite region. It is noted that lubrication during ferritic rolling has been identified as an important factor in order to produce a homogeneous through-thickness microstructure.

Mechanical Properties of Niobium-Bearing Interstitial-Free Steels

Interstitial-free steels have found many applications due to improved formability characteristics when compared to typical low carbon steel grades. The lack of a yield point, the enhanced work hardening characteristics, and the improved drawability are all important product attributes of interstitial-free steels. Additionally, interstitial-free steels have a high strain rate sensitivity, as shown in Figure 7.

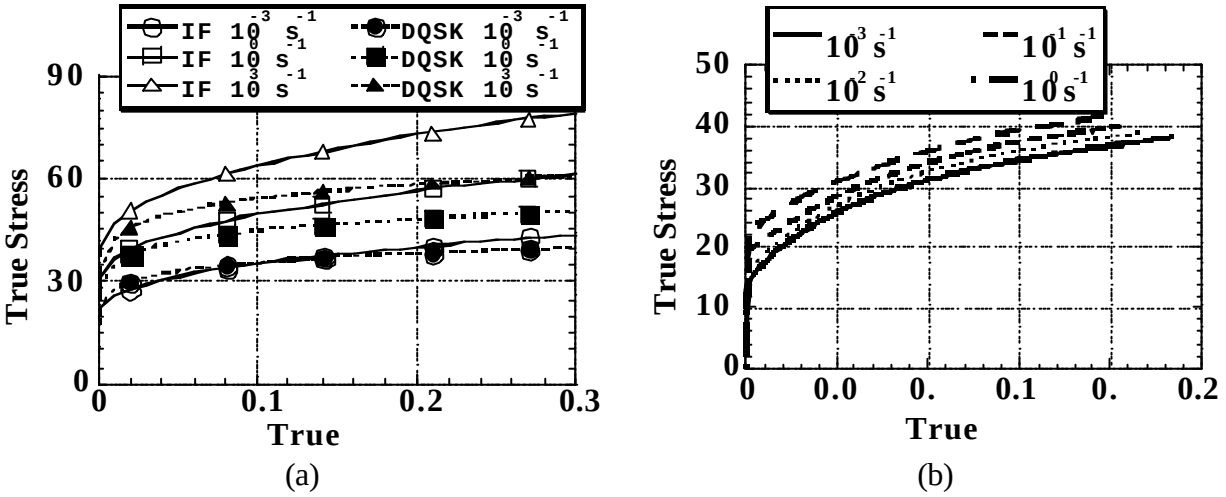

Figure 7: a) Predicted True Stress-True Strain Curves for Interstitial-Free (IF) and DQSK Steels at strain rates of 10^{-3} (quasi-static), 10^{0} (stamping), and 10^{3} (crash event) based upon Johnson-Cook curve fits (81) and b) Experimental True Stress-True Strain Curves for a TiNb-stabilized steel (data courtesy of T. M. Link-U. S. Steel).

Table I displays representative property targets for interstitial-free steels for the automotive industry. The properties of a typical "standard" TiNb-stabilized steel are shown in Table II. The properties of this grade meet many applications, but as can be seen in Table I, there are applications that require either higher strength levels or increased formability characteristics. Figure 8 and Table IV displays two routes that can be taken to increase the strength of interstitial-free steels: i) heavy temper rolling and ii) alloying. Increasing the amount of temper extension will increase the strength of the sheet; however, there will be a decrease in formability. While this method can be used to strengthen TiNb-stabilized steels, the prescribed

temper extension is typically more related to shape and surface appearance than to strengthening.

Table I Representative property targets for interstitial-free steels (82-84) (0.8 mm sheet)

Yield Strength (MPa)	**Tensile Strength (MPa)**	**Total Elongation (percent)**	**n-value (between 10% & 20% strain)**	**r_m-values**
110 min.	270 min.	42 min. [A]	0.22 min.	1.7 min.
110 min.	270 min.	45-55 [JL]		>1.5
120 min.	270 min.	43-53 [JL]		>1.4
125 min.	270 min.	41-51 [JL]		>1.2
140 min.	270 min.	40 min. [A]	0.20 min.	1.6 typical
180 min.	310 min.	40 min. [A]	0.20 min.	1.7 typical
210 min.	330 min.	38 min. [A]	0.19 min.	1.7 typical
210 min.	340 min.	36-46 [JT]		>1.3
255 min.	390 min.	32-43 [JT]		>1.3
310 min.	440 min.	28-39 [JT]		>1.2

[A] – ASTM longitudinal specimen, [JL] = JIS longitudinal specimen,
[JT] – JIS transverse specimen (note: JIS elongaton $\geq$ 1.10 ASTM elongation, typically).

Table II Properties from a typical "standard" TiNb-stabilized steel. (PRO-TEC Coating Company, March 2001, 271 tests)

Composition in weight percent				
C	N	S	Ti	Nb
0.005 max	0.006 max.	0.012 max.	0.025 / 0.045	0.025 / 0.045

Properties			
Yield Strength (MPa)	Tensile Strength (MPa)	n-value	Elongation (percent)
147 $\pm$ 7.3	306 $\pm$ 10	0.236 $\pm$ 0.006	45.8 $\pm$2.5

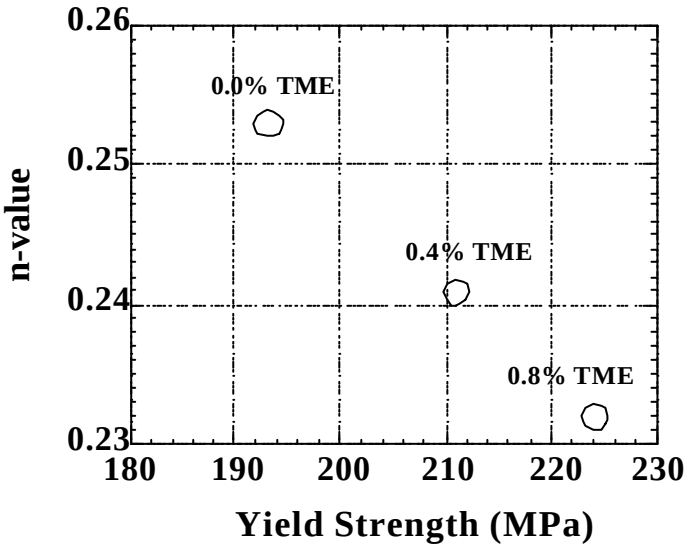

Figure 8: The effect of temper rolling (TME = temper mill extension) on properties of a TiNb-stabilized steel

Table III Effect of alloying for strengthening (change in each property with an incremental change in compostion) (85).

Change in Composition (weight percent)	Yield Strength (MPa)	Tensile Strength (MPa)	Uniform Elongation (percent)	Total Elongation (percent)
0.1 Si	9.7	13.3	-0.52	- 0.85
0.1 Mn	2.7	3.4	-0.28	-0.34
0.01 P	3.5	7.1	-0.38	-1.2

Table IV Effect of composition (wt. pt.) on secondary work embrittlement.

C	N	Ti	Nb	P	Mn	Si	B	DBTT (°C)
0.0026	0.0029	0.010	0.023	0.080	0.17	0.20	-	- 30 (87)
0.0027	0.0023	0.012	0.024	0.079	0.33	0.63	-	- 5 (87)
0.0024	0.0028	0.010	0.022	0.080	0.17	0.20	0.0009	< -70 (87)
0.0022	0.0030	0.011	0.024	0.080	0.35	0.70	0.0014	- 40 (87)
0.0036	0.0035	0.06	-	0.014	0.16	-	-	- 40 (88)
0.0033	0.0037	0.03	0.03	0.014	0.16	-	-	- 60 (88)
0.0035	0.0031	0.06	-	0.06	0.16	-	-	+ 10 (88)
0.0036	0.0035	0.06	0.03	0.06	0.16	-	-	- 20 (88)

Most often, alloying additions are made to the base interstitial-free steel in order to produce solid solution strengthening. Phosphorus, manganese, and silicon additions are made according to the relationships shown in Table IV. The choice of alloying element, or combinations of alloying elements, for interstitial-free steels is made in light of the effects of each element on mechanical properties and on compatibility with hot-dip coating. The effect of each of the alloying elements on hot-dip galvanneal coating will be discussed in the next section. With regard to mechanical properties, phosphorus is the most potent strengthening element and is often employed in higher strength grades.

While phosphorus is very effective in increasing the strength of interstitial-free steels, phosphorus-bearing grades may exhibit secondary work embrittlement after deep drawing (86, 87). This phenomenon involves the brittle fracture of a deformed sample upon subsequent loading. The resistance of a steel to secondary work embrittlement is most often described by a ductile to brittle transition temperature (DBTT). One method of determining the DBTT utilizes drawn cups that are deformed at a series of temperatures using a drop weight test. The fracture type is macroscopically defined as ductile or brittle and the DBTT shown in Table IV is defined as the temperature at which brittle fracture is a prevalent failure mode*.

Evaluations of cups that fail in a brittle fashion reveal a predominance of intergranular fracture. This fracture mode is favored due to the absence of carbon at the grain boundaries coupled with the grain boundary segregation of phosphorus. While solute niobium at the grain boundaries may reduce the tendency for secondary work embrittlement, boron additions are typically made to phosphorus-bearing TiNb-stabilized steels in order to improve the resistance to secondary work embrittlement.

Boron additions promote a transition from intergranular fracture to ductile tearing, resulting in a marked decrease in the DBTT shown in Table IV. The rapidly diffusing boron segregates to

* For example, one testing procedure defines the DBTT as the temperature at which 25 percent of the cups tested exhibit brittle fracture after a minimum of eight cups are tested at that temperature.

grain boundaries, increases the cohesive strength, and effectively compensates for the absence of carbon and the presence of phosphorus. It is noted that boron additions will result in an increase in the recrystallization temperature as well as an increase in strength (approximately 4 MPa per 0.001 weight percent (85)).

Thus far, the discussion has focused on higher strength interstitial-free steels. As shown in Table I, there are also commercial applications for grades with improved formability characteristics. Figure 9 summarizes some of the methods that can be utilized to increase elongation and drawability (i.e., r_m-value). One of the important tactics utilized to increase the ductility of interstitial-free steels is to decrease the total nitrogen and carbon contents via optimization of steelmaking techniques. Decreasing the total carbon content also decreases the amount of niobium necessary for stabilization and further promotes increased ductility (see Figure 9b).

Increasing the annealing temperature will increase the elongation and r_m-value of TiNb-stabilized steels. It is important to note, however, that the annealing temperature must remain below the carbide dissolution temperature to prevent the introduction of solute carbon, which may degrade formability[**]. In addition to annealing temperatures, the r_m-value is related to cold reduction and typically reaches a maximum between 75 and 85 percent cold reduction.

Hot strip mill processing will also influence the properties of TiNb-stabilized steels. In order to produce a more ductile final product, the goal of hot strip mill processing is to produce coarse precipitates and equiaxed grains. The reheat temperature and the alloy content will determine the extent of carbide dissolution. Lower reheat temperatures and sufficient alloying (i.e., $K > K_{sp}$) will favor coarse precipitates and polygonal ferrite. Additionally, lower reheat temperatures may result in the formation of $(Ti,Nb)_4C_2S_2$ precipitates, which have been proposed to improve ductility (24-28).

Finishing temperature has a marked effect on rm for TiNb-stabilized steels. Gupta, et al. (61) found that r_m-value of the final cold rolled sheet increases with increasing finishing temperature up to 900 ^oC. At the higher finishing temperatures, a homogeneous, equiaxed microstructure is favored. Lowering the finishing temperature results in a mixed microstructure and a more random hot band texture, both of which being detrimental to texture development in the final cold rolled sheet. As a result, higher finishing temperatures are typically favored. It is noted that the use of higher finishing temperatures often dictates the use of higher reheat temperatures in commercial production.

The coiling temperature is very important for property development. Tokunaga, et al. (89) observed an increase in elongation and r_m-value with an increase in coiling temperature. For example, elongation was found to increase from 44 to 46 percent and r_m-value from 1.6 to 2.0 with an increase in coiling temperature from 600 ^oC to 720 ^oC for a 0.02 weight percent Nb grade. The primary reason for this increase is the coarser precipitates that form during cooling of the coil.

[**] It is also noted that carbide dissolution at higher annealing temperatures is a potential production technique for bake-hardenable steels, which rely upon solute carbon for strengthening.

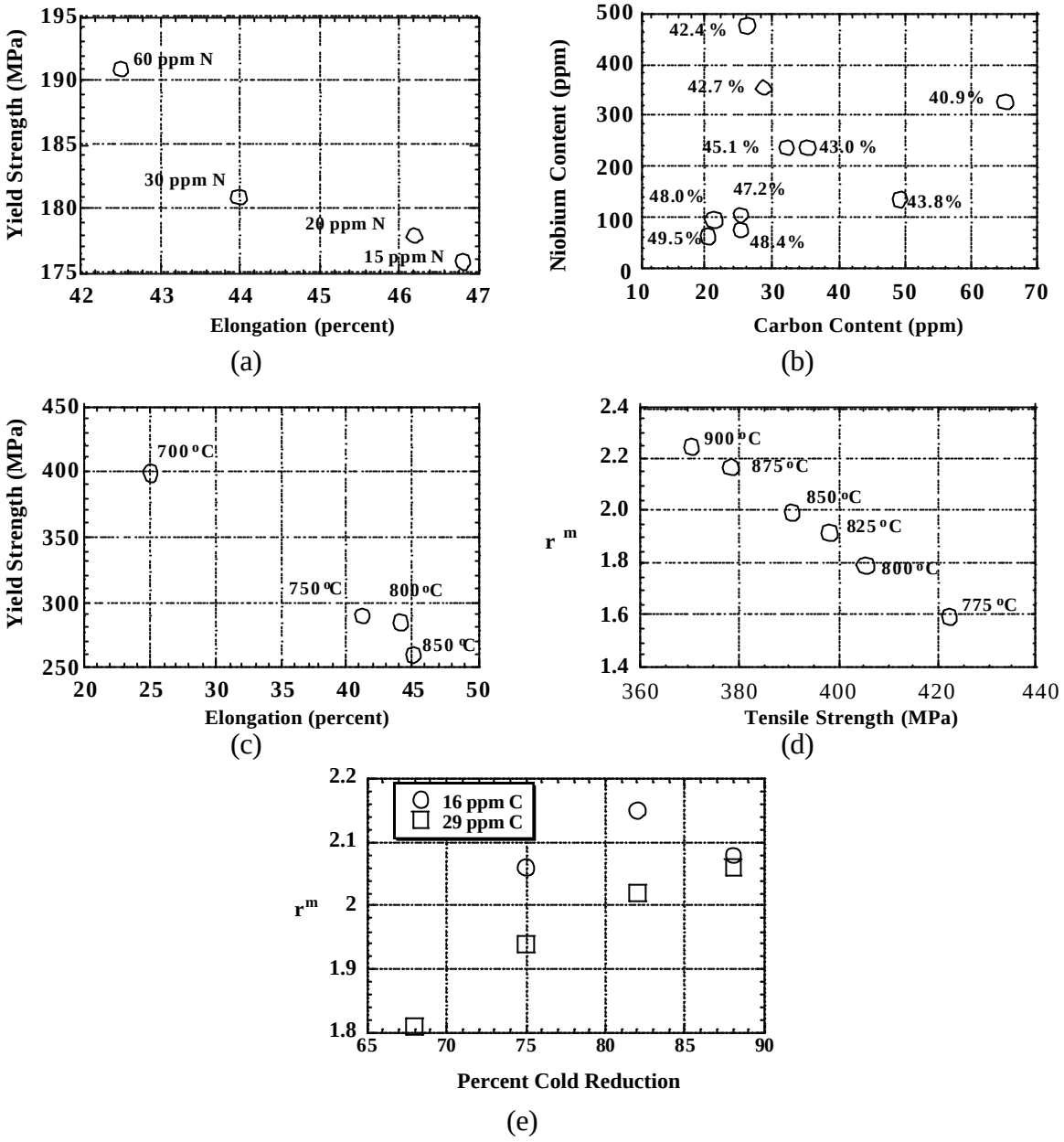

Figure 9: Summary of Property Trends: a) Effect of nitrogen content on yield strength and elongation (TiNb steel)[89], b) Effect of carbon and niobium content on elongation (TiNb steel)[89], c) Effect of annealing temperature on yield strength and elongation (Ti-Nb-P-Mn-Si-B grade)[90], d) Effect of annealing temperature on tensile strength and r_m (Ti-Nb-0.5Mn grade)[91] and e) Effect of cold reduction on rm (Ti-Nb-0.5Mn grade) (91).

The above discussion assumes traditional austenitic hot rolling. Recently, the use of lubricated ferritic rolling has been investigated for the enhancement of r_m-value (92,93). This practice has been found to increase the r_m-value by greater than 0.5, even leading to the production of cold rolled sheet with an r_m-value of 3.0. The use of lubrication promotes a more uniform strain across the cross-section, resulting in a more uniform microstructure. Ferritic rolling facilitates a stronger {111} texture, which when coupled with higher annealing temperatures, promotes a marked increase in r_m-value.

All of these techniques could be used to promote increased ductility; however, it should be noted that a TiNb-stabilized steel will typically have a lower ductility than a Ti-stabilized steel. This is primarily related to the grain refinement and finer precipitate distribution in niobium-bearing grades. As a result, applications requiring the highest degree of ductility typically utilize titanium for stabilization, employ low carbon and nitrogen contents, utilize higher coiling and annealing temperatures, and contain minimal niobium additions. The primary reason for niobium additions in these grades is related to the role of niobium in the hot-dip galvannealing process, which is discussed in the following section.

Hot-Dip Galvanneal Coating of Niobium-Bearing Interstitial-Free Steels

As stated previously, the commercial utilization of niobium-bearing interstitial-free steels is primarily for hot-dip galvanneal coated sheets. Hot-dip galvanneal coatings are iron-zinc alloy coatings, which typically contain between 8 and 12 weight percent iron. These coatings have been developed primarily for increased corrosion resistance as well as increased weldability.

The galvannealing process involves coating steel in a zinc bath with a low aluminum content (typically less than 0.15 weight percent) followed by processing through a furnace at 460 ^{o}C to 540 ^{o}C. The elevated temperatures promote the interdiffusion of iron and zinc, resulting in the iron-zinc alloy coating. As shown in Figure 10a, the galvanneal coating contains layers of iron-zinc phases.

Microstructural evolution during this process begins with the formation of an iron-aluminum-zinc intermetallic layer, typically called an inhibition layer. In order for the galvanneal structure to form, holes in the inhibition layer must exist or the layer must be broken to allow for the interdiffusion of iron and zinc[*]. Intimate contact between zinc and iron results in the formation of iron-rich phases, which grow into the zinc-rich coating as shown in Figure 10b. In general, the rate of phase formation and the final coating microstructure will be dependent upon the bath composition, the thermal profile beginning at bath entry and continuing through the galvannealing furnace, and the steel type.

The overall properties of the coating will be related to the amount of each phase present in the coating and the characteristics of each phase (see Table IV). In general, minimization of the brittle Γ/Γ_1 layer thickness is preferred as coating adherence is degraded as the thickness of this layer increases. For a fully-galvannealed coating (i.e., one without "free-zinc" or η-phase), the phases at the surface of the sheet will be either the soft ζ-phase or the hard δ-phase. The relative amounts of these two phases will therefore influence the frictional characteristics of the sheet.

During the commercial development of galvanneal-coated interstitial-free steels, coating adherence was a key performance variable[**]. Through the use of a Taguchi experimental matrix, Zeik, et al. (94) illustrated that the stabilization technique had a larger effect on coating adhesion than other processing variables. In particular, TiNb-stabilized steels had better coating adherence than Ti-stabilized steels. The improved coating adherence of TiNb-stabilized steels when compared to Ti-stabilized steels has been similarly documented in studies investigating powdering behavior (see Figure 11) and interfacial strength (95-97).

---

[*] It is noted that low bath aluminum contents are needed. If the aluminum content is too high, the inhibition layer will not "breakdown" and will retard the formation of the galvanneal structure.

[**] The variables studied in this study were steel type (Ti-stabilized versus TiNb-stabilized,), bath aluminum, strip entry temperature, galvanneal furnace temperature, line speed, and cooling after galvannealing.

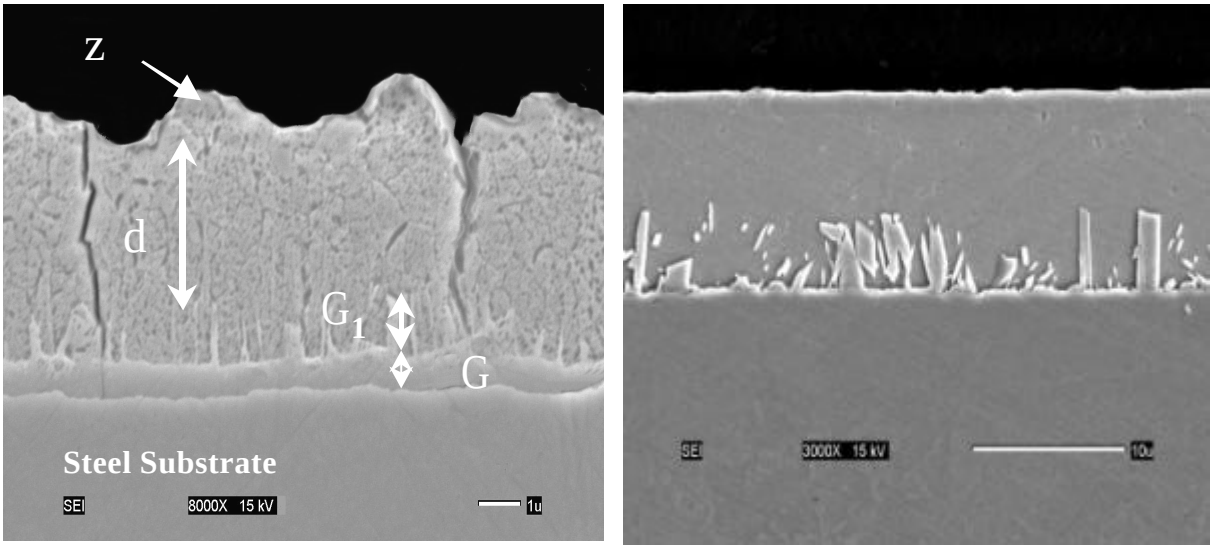

(a) (b)

Figure 10: a) Cross-section of a hot-dip galvanneal coating and b) the initial stages of the galvannealing process. Micrographs courtesy of M. Simko and E. A. Silva - U. S. Steel.

Table IV Iron-Zinc Phases in Typical Hot-Dip Galvanneal Coatings

Phase	Weight Percent Iron	Characteristic
η (Zn)	0	Ductile
ζ ($FeZn_{13}$)	5 – 6	Ductile
δ ($FeZn_7$)	7 – 12	Brittle
Γ ($FeZn_4$)	17 – 22	Brittle
Γ_1 (Fe_3Zn_{10})	15 - 28	Brittle

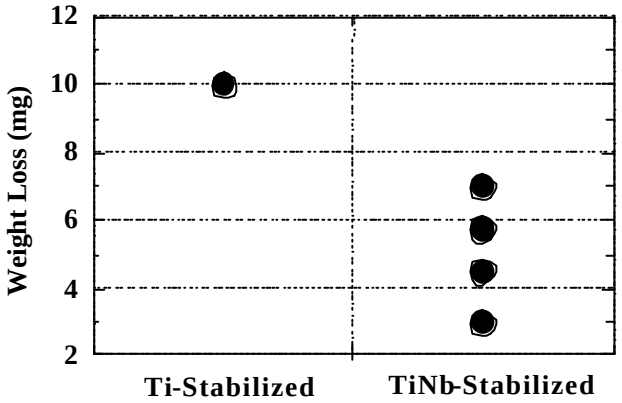

Figure 11: Comparison of the weight loss in Double Olsen testing between Ti-stabilized and TiNb-stabilized steels (95).

The difference in coating adherence observed in these studies is a result of the microstructural development of the galvanneal coatings. Due to the removal of carbon from solution in the substrate, the penetration of zinc at grain boundaries will be more rapid than in non-stabilized steels, resulting in an increased reactivity during galvannealing. The rapid penetration of zinc leads to the formation of "outbursts", which are essentially regions of more rapid alloy growth (98, 99). While this outburst phenomenon occurs for both types of steels, Ti-stabilized grades exhibit a higher propensity for outbursts than TiNb-stabilized grades. As a result, the growth of

iron-rich phases is more rapid for Ti-stabilized steels than for TiNb-stabilized steels, resulting in a deleterious increase in the thickness of the $\Gamma/\ \Gamma_1$-layer.

The difference in galvanneal structure for Ti-stabilized and TiNb-stabilized steels begins in the initial stages of galvannealing. Fujibayashi, et al. (100) found that the breakdown of the inhibition layer for Ti-stabilized steels occurred randomly, but was more uniform for TiNb-stabilized steels. McDevitt, et al. (101) found that the initial formation of the ζ-phase for Ti-stabilized steels occurred without a preferred orientation. By comparison, the ζ-phase for TiNb-stabilized steels grew in one direction and had a "colony" size that was similar to the substrate grain size. Likewise, Carless, et al. (97) found that nucleation of the ζ-phase in TiNb-stabilized steels preferentially occurred over (111) α-iron, resulting in a lower consumption of iron and a correspondingly slower growth rate for the iron-rich $\delta-$ and $\Gamma-$phases. After initiation of alloying, the presence of solute niobium at the grain boundaries may also serve to decrease the intergranular diffusion of iron, thus assisting in the production of a more uniform alloy structure with a reduced $\Gamma-$layer thickness.

In addition to alloy phase development, niobium additions are also beneficial for the reduction of "woodgrain" appearance on the surface of the galvanneal sheet. This pattern of light and dark streaks is frequently observed in grades with high titanium content (102) and is typically associated with hot strip mill scale. The use of niobium for interstitial stabilization therefore reduces the necessary titanium content in the sheet, thus reducing the propensity for this type of surface appearance.

Microstructural development also plays an important role in the galvannealing of high strength interstitial-free steels. As mentioned previously, phosphorus additions are commonly made to TiNb-stabilized steels in order to achieve higher strength levels. When processing these grades, however, it has been found that higher temperatures and/or longer times are needed to produce a fully galvannealed coating. The addition of phosphorus dramatically reduces the amount of outbursts that occur (98, 103), resulting in a reduction in the overall alloy growth rate. This decrease in galvannealing kinetics has been primarily attributed to the reduced interdiffusion of zinc and iron due to grain boundary segregation of phosphorus. Additionally, the surface segregation of phosphorus may also serve to retard breakdown of the inhibition layer (104). As a result, phosphorus-bearing grades typically have a minimal amount of $\Gamma-$phase.

Manganese additions may also be made to increase the strength of interstitial-free steels. An important consideration for hot-dip galvannealing of grades with high manganese contents is the oxidation potential of manganese. As shown in Figure 12, manganese has a lower oxidation potential than iron and will therefore be more readily oxidized, especially at higher alloy contents. As shown in Figure 12b, the equilibrium dew point for manganese in steel is lower than that for iron. As a result, a dew point that is reducing for iron may be oxidizing for manganese, resulting in the formation of manganese oxides on the surface. The wettability of the steel surface by zinc is reduced by the presence of manganese oxides and can lead to bare spots on the surface of the sheet. As a result, control of the dew point during annealing becomes important. It is noted, however, that manganese may have a beneficial effect on galvannealing by reducing the activity of phosphorus at the grain boundaries (105). This effect, however, is most notable in conjunction with internal oxidation in highly oxidizing atmospheres, which subsequently requires processing in a highly reducing environment to facilitate wetting and galvannealing.

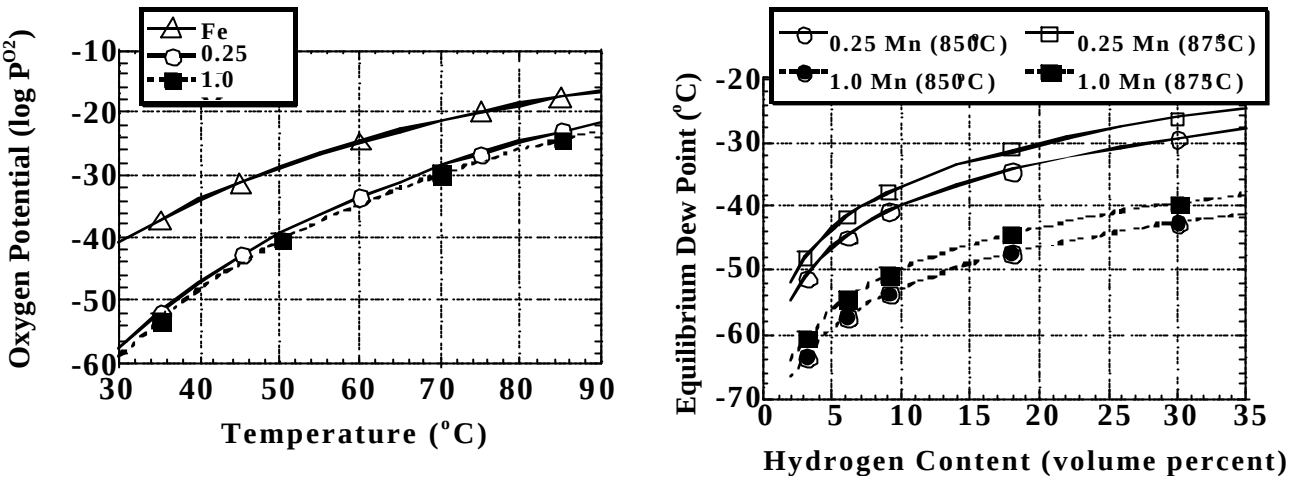

(a) (b)

Figure 12: a) Comparison of the oxygen potential for iron, 0.25 weight percent manganese, and 1.0 weight percent manganese and b) the equilibrium dew points for 0.25 weight percent manganese, and 1.0 weight percent manganese in a 0.004C-0.003N-0.008S-0.035Si grade. (Assumes the activity of manganese equals the atomic fraction and 1.0 atm total pressure).

Silicon is also a potential strengthening element for interstitial-free steels. Silicon is much more readily oxidized than manganese. For example, the oxidation potential for 0.035 and 0.30 weight percent silicon at 850 °C is –59.4 and -61.3, respectively. Silicon oxide is typically non-wetting and therefore will result in bare spots in the galvanneal coating. The formation of complex oxides may, however, be less detrimental to the galvanneal coating. In laboratory experiments, Kato (106) has found that fewer bare spots are observed when $MnSiO_3$ forms on the surface of steel during annealing than when SiO_2 or Mn_2SiO_4 form.

As mentioned previously, boron additions may also be made to phosphorus-bearing interstitial-free steels to improve the resistance to secondary work embrittlement. Phase development for boron-bearing grades is much slower than for base TiNb-stabilized grades (107). This reduction in galvannealing kinetics is most likely related to the presence of phosphorus and boron at the grain boundaries as well the surface segregation of boron.

Summary

The production and properties of TiNb-stabilized steels have been reviewed. In order to achieve the good formability characteristics typical of interstitial-free steels, modern steelmaking and casting practices are utilized to minimize the total nitrogen and carbon content in the steel. The remaining interstitial nitrogen and carbon are removed from solid solution via precipitation, predominantly as TiN, $(Ti, Nb)_4C_2S_2$, TiC, or NbC. The amount and type of precipitate will be determined by the composition of the steel and the thermomechanical processing procedures.

A standard TiNb-stabilized steel will exhibit enhanced formability characteristics when compared to low carbon steels. The ductility of these grades can be further enhanced through proper selection of thermomechanical processing and via the minimization of nitrogen and carbon contents. The strength of TiNb-stabilized steels can be effectively increased through

solid solution strengthening; however, alloy design for higher strength grades will typically include boron additions as a means to increase the resistance to secondary work embrittlement.

Many commercial applications of niobium-bearing interstitial-free steels involve hot-dip galvanneal coatings. TiNb-stabilized steels exhibit better coating adhesion than Ti-stabilized steels. This is primarily attributable to retardation of the interdiffusion of iron and zinc at the ferrite grain boundaries and the nucleation of favorably oriented ζ-phase, both of which allow for a more uniform galvanneal microstructure. The production of higher strength grades for hot-dip galvanneal coatings is highly dependent upon the effect of the alloying elements on the interdiffusion of iron and zinc as well as the oxidation potential of the alloying elements.

Acknowledgements

Useful discussions with Ed Silva, Dennis Haezebrouck, and Jesus Jimenez of U. S. Steel are gratefully acknowledged.

References

(1) C. A. Edwards, D. L. Phillips, H. N. Jones, "The Influence of Some Special Elements Upon the Strain-Ageing and Yield-Point Characteristics of Low-Carbon Steels", J. Iron and Steel Inst., 142 (1940), 199-236.

(2) I. Codd and N. J. Petch, "Dislocation-locking by Carbon, Nitrogen, and Boron in α-Iron", Phil. Mag., 5 (1960), 30-42.

(3) R. E. Hook, " The Effect of Quench-Aging on Inhomogeneous Yielding of Steels with Very Low Interstitial Solute Content", Metall. Trans., 1 (1970), 85-92.

(4) W. C. Leslie and R. J. Sober, "Yielding and Plastic Flow in a Polycrystaline "Interstitial-Free" Fe-0.15% Ti Alloy", Trans. ASM, 60 (1967), 99-111.

(5) W. C. Leslie, "Iron and Its Dilute Substitutional Solid Solutions", Metall. Trans., 3 (1972), 5-26.

(6) R. E. Hook and J. A. Elias, "The Effect of Composition and Annealing Conditions on the Stability of Columbium-Treated Low Carbon Steels", Metall. Trans., 3 (1972), 2171-2181.

(7) T. W. Miller, J. Jimenez, A. Sharan, and D. A. Goldstein, "Oxygen Steelmaking Processes", The Making Shaping and Treating of Steel, 11th edition, ed. R. J. Fruehan, (AISE Foundation, Pittsburgh, PA, 1998), 475-524.

(8) E. T. Turkdogan and R. J. Fruehan, "Fundamentals of Iron and Steelmaking", The Making Shaping and Treating of Steel, 11th edition, ed. R. J. Fruehan, (AISE Foundation, Pittsburgh, PA, 1998), 13-157.

(9) P. Nilles, P. Dauby, and J. Claes, "Physical Chemistry of Top and Bottom Blowing", Basic Oxygen Steelmaking, (The Metals Society, London, 1979), 60-72.

(10) G. J. W. Kor and P. C. Glaws, "Ladle Refining and Vacuum Degassing", The Making Shaping and Treating of Steel, 11th edition, ed. R. J. Fruehan, (AISE Foundation, Pittsburgh, PA, 1998), 661-713.

(11) M. Takahashi, H. Matsumoto, T. Saito, "Mechanism of Decarburization in RH Degasser", ISIJ Intl., 35 (1995), 1452-1458.

(12) Y. Kishimoto, Y. Yamaguchi, T. Sakuraya, T. Fuji, "Decarburization Reaction in Ultra-low Carbon Iron Melt Under Reduced Pressure", ISIJ Intl., 33 (1993), 391-399.

(13) F. Stouvenot, F. Chatelain, D. Huhin, "Kinetics of Decarburization of ULC Steels in Vacuum Tank Degasser at Sollac Florange", proc. 39th Mechanical Working and Steel Processing Conference, (Iron and Steel Society, Warrendale, PA, 1998), 283-288.

(14) W. Van Der Knoop, W. H. L. Moonen, J. Post, G. Van Unene, "Nitrogen Control in Liquid Steel for Slab Casting", La Revue de Metallurgie-CIT, April 1995, 503-510.

(15) T. Kuwabara, T. Hiraoka, T. Nuibe, H. Fujii, S. Tanaka, "Production of Interstitial-Free Steel Slab", proc. 70th Steelmaking Conference, (Iron and Steel Society, Warrendale, PA, 1987), 381-387.

(16) P. J. Koros, "Pre-Treatment of Steels", The Making Shaping and Treating of Steel, 11th edition, ed. R. J. Fruehan, (AISE Foundation, Pittsburgh, PA, 1998), 413-429.

(17) Metallurgy of Continuous-Annealed Sheet Steel, eds. B.L. Bramfitt and P.C. Mangonon, Jr., (TMS-AIME, Warrendale, PA, 1985).

(18) Technology of Continuously Annealed Cold-Rolled Sheet Steel, ed. R. Pradhan, (TMS-AIME, Warrendale, PA, 1985).

(19) Metallurgy of Vacuum-Degassed Steel Products, ed. R. Pradhan, (TMS-AIME, Warrendale, PA, 1990).

(20) Interstitial-Free Steel Sheet: Processing, Fabrication and Properties, Proc. Int. Symp., eds .L.E. Collins and D.L. Baragar, (Canadian Institute of Mining, Metallurgy and Petroleum, Ottawa, 1991).

(21) International Forum for Physical Metallurgy of IF Steels, The Iron and Steel Institute of Japan, and Nissho Iwai Corporation, Tokyo, 1994.

(22) R.E. Hook and H. Nyo , "Recrystallization of Deep Drawing Columbium (Nb)-Treated Interstitial-Free Sheet Steels", Metall. Trans. A, 6A (1975), 1443-1451.

(23) K. Sato and Y. Ishiguro, "Microchemistry of Complex Carbides", International Forum for Physical Metallurgy of IF Steels, ISIJ, Tokyo, 1994, 45-48.

(24) M. Hua, C.I. Garcia, and A.J. DeArdo, "Precipitation Behavior in Ti-only, Ti+Nb Dual Stabilized and Nb-Only Ultra-Low Carbon Interstitial-Free Steels", Proc. Int. Symp. Phase Transformations during the Thermal/Mechanical Processing of Steel, eds. E.B. Hawbolt and S. Yue, (TMS-CIM, Vancouver, 1995), 285-290.

(25) M. Hua, C.I. Garcia, and A.J. DeArdo, "Multi-Phase Precipitates in Interstitial-Free Steels", Scr. Metall. Mater., 28 (1993), 973-978.

(26) M. Hua, C.I. Garcia, and A.J. DeArdo, Int. Symp. on Low-Carbon Steels for the 90's, eds. R. Asfahani and G. Tither, (TMS-AIME, Warrendale, PA, 1993), 445-451.

(27) G. Tither, C.I. Garcia, M. Hua, and A.J. DeArdo, "Precipitation Behavior and Solute Effects in Interstitial-Free Steels Sheets", International Forum for Physical Metallurgy of IF Steels, ISIJ, Tokyo, 1994, 293-322.

(28) A.J. DeArdo, "Multi-Phase Microstructures and Their Properties in High Strength Low Carbon Steels", ISIJ Int., 35 (1995), 946-954.

(29) A. Okamoto and N. Mizui, "Texture Formation in Ultra-Low-Carbon Ti-added Cold-Rolled Sheet Steels containing Mn and P", in Metallurgy of Vacuum-Degassed Steel Products, (TMS-AIME, Warrendale, PA, 1990), 161-180.

(30) S. Satoh, T. Obara, and K. Tsunoyama, Trans. Iron Steel Inst. Jpn., 26 (1986), 737-744.

(31) K. Tsunoyama, K. Sakata, T. Obara, S. Satoh, K. Hashiguchi, and T. Irie, "Effect of Lowering Sulfur Content in Ti-added, Deep Drawable Hot- and Cold-Rolled Sheet Steels", Hot- and Cold-Rolled Sheet Steels, (TMS-AIME, Warrendale, PA, 1988), 155-164.

(32) W.J. Liu, S. Yue, and J.J. Jonas , "Characterization of Ti Carbosulfide Precipitation in Ti Microalloyed Steels", Metall. Trans. A, 20A (1989), 1907-15.

(33) S.V. Subramanian, M. Prikryl, A. Ulabhaje, and K. Balasubramanian, Interstitial-Free Steel Sheet: Processing, Fabrication and Properties, (Canadian Institute for Mining, Metallurgy and Petroleum, Ottawa, 1991), 15-38.

(34) M. Yoshinaga, K. Ushioda, S. Akamatsu, and O. Akisue, ISIJ Int., 34 (1994), 24-32.

(35) K. Balasubramanian, and J. S. Kirkaldy, "Thermodynamics of Fe-Ti-C and Fe-Nb-C Austenites and Nonstoichiometric Titanium and Niobium Carbides," Advances in Phase Transitions, ed. J.D. Embury and G.R. Purdy, (Pergamon Press, Oxford, UK, 1988), 37-51.

(36) A. J. DeArdo, "Physical Metallurgy of Interstitial-Free Steels: Precipitates and Solutes", IF Steel 2000, (ISS, Warrendale, PA, 2000), 125-136.

(37) M. Phadke, M.S. Thesis, University of Pittsburgh, 1998.

(38) G. Dupuis, R.A. Hubert, and R. Taillard, "A Detailed Study of Sulphide Precipitation in Ti-IF Steels", proc. 40th Mechanical Working and Steel Processing Conference Proceedings, (ISS, Warrendale, PA, 1998) 117-125.

(39) R.E. Hook, “Effect of Cb on the Development of Recrystallization Textures in Cb-Treated Interstitial-Free Steels,” Metallurgy of Vacuum-Degassed Steel Products, ed. R. Pradham, (TMS-AIME, Warrendale, PA, 1990), 263-287.

(40) R.E. Hook, A.J. Hecker, and J.A. Elias, “Texture in Deep Drawing Columbium (Nb)-Treated Interstitial- Free Steels,” Metall. Trans. A, 6A (1975), 1683-1692.

(41) W.B. Hutchinson, K. I. Nilsson and J. Hirsch, “Annealing Texture in Ultra-Low Carbon Steels,” Metallurgy of Vacuum-Degassed Steel Products, Ed. R. Pradhan, (TMS-AIME, Warrendale, PA, USA, 1990), 57-61.

(42) . Gillanders, C. Dasarathy, and R. C. Hudd, “Some Observations on the Development of Deep Drawing Characteristics in Low Carbon Steels Containing 0.07 to 0.27 wt% Niobium,” Proc. 4th Int. Conf on Textures and Properties of Materials, Eds. G. J. Davies, I. L. Dillamore, and R. C. Hudd, (Institute of Metals, London, 1975, Published in 1976), 245-254.

(43) D. J. Willis and M. Hatherly, “Texture Development in Niobium Stabilized Steel Sheet,” Proc. 4th Int. Conf on Textures and Properties of Materials, Eds.G. J. Davies, I. L. Dillamore, and R. C. Hudd, (Institute of Metals, London, 1975, Published in 1976), 48-53.

(44) S. Satoh, T. Obara, M. Nishida and T. Irie, “Effects of Alloying Elements and Hot-Rolling Conditions on the Mechanical Properties of Continuously Annealed Extra-Low Carbon Steel Sheet,” Technology of Continuously Annealed Cold-Rolled Sheet Steel, Ed. R. Pradhan, (AIME, Warrendale, PA, 1984), 151-166.

(45) S. D. Hole, W. T. Roberts, and D. V. Wilson, “The Effect of Hot-Band Structure on Texture Development in Low-Carbon Steel Sheet,” Metal Science, 8 (1974), 277-285.

(46) L.J. Ruiz-Aparicio, "Development of Crystallographic Texture in Ultra-Low Carbon Sheet Steel", Ph.D. Dissertation, School of Engineering, University of Pittsburgh, 1998.

(47) R.K. Ray and J. J. Jonas, "Transformation Textures in Steels", Int. Mat. Rev., 35 (1) (1990), 1-36.

(48) P.H. Chapellier, et al., "Prediction of Transformation Textures in Steels", Acta Metall. Mater., 38 (8) (1990), 1475-1490.

(49) M. Lamberiguts and T. Greday, "Mechanisms Operative During Hot Rolling and Cooling of HSLA Steels", The Hot Deformation of Austenite, ed. Balance, J.B., (1977), 286-315.

(50) R. Coladas, J. Masounave, and J. P. Ballon, The Hot Deformation of Austenite, ed. Balance, J.B., (1977), 341-383.

(51) J. J. Jonas, et al., "Effect of Precipitation on Recrystallization in Microalloyed Steels", Metal Science, 13 (1979), 238-245.

(52) I. Weiss, et al., "Interaction Between Recrystallization and Precipitation During the High Temperature Deformation of HSLA Steels", Metall. Trans., 10A (1979), 831-840.

(53) R. K. Ray, et al., "Effect of Controlled Rolling on Texture Development in a Plain Carbon and a Nb Microalloyed Steel", ISIJ Int., 32 (2) (1992), 203-212.

(54) R. K. Ray, J. J. Jonas, and R. E. Hook, "Cold Rolling and Annealing Textures in Low Carbon and Extra Low Carbon Steels", Int. Mat. Rev., 39 (7) (1994), 129-172.

(55) U. Schlippenbach, F. Emren, and K. Lucke, "Investigation of the Development of the Cold Rolling Texture in Deep Drawing Steels by ODF-Analysis", Acta Metall., 34 (7) (1986), 1289-1301.

(56) D. O. Wilshynsky, D. K. Matlock, and G. Kranss, "Microstructure and Mechanical Properties of Interstitial-Free Steel Sheet Steels with Different Stabilizing Additions", Metallurgy of Vacuum-Degassed Steel Products, Indianapolis, Oct. 3-5, 1989, (TMS, Warrendale, PA, 1990), 247-287.

(57) H. Inagaki, "Transformation Textures in Control-rolled High Tensile Strength Steels", Trans. ISIJ, 17 (1977), 166-173.

(58) H. Inagaki, Z. Metallkde, 74 (1983), 716.

(59) R. E Hook, "Physical Asymmetry of the Crystallographic texture of an Interstitial-Free Sheet Steel", Metall. Trans., 24A (1993), 2009-2019.

(60) I. Gupta and D. Bhattacharya, "Metallurgy of Formable Vacuum Degassed Interstitial-Free Steels", Metallurgy of Vacuum Degassed Steels, (TMS, Warrendale, PA, 1990), 43-72.

(61) I. Gupta, T. Parayil, and L.-T. Shiang, "Effect of Processing Parameters on the Properties of Cold Rolled Interstitial-Free Steels", Hot- and Cold-Rolled Sheet Steels, (TMS, Warrendale, PA 1988), 139-153.

(62) S. Satoh, "A New Process for Manufacturing Deep-Drawing Cold Rolled Steel Sheets from Extra Low Carbon Steels", KSC Report, 1985, 36-44.

(63) Y. Furono, "Effect of Hot Rolling in Ferrite Phase on the Mechanical Properties of Very-Low Carbon Titanium Cold Rolled Sheet Steels", Tetsu-To-Hagne, 71 (13) (1985), S1362.

(64) S. Satoh, T. Obara, M. Nishida and T. Irie, Technology of Continuously Annealed Cold Rolled Sheet Steel, "Effects of Alloying Elements and Hot Rolling Conditions on the Mechanical Properties of Continuous Annealed Extra-Low-Carbon Steel Sheet", (TMS-AIME, Warrendale, PA, 1985), 151-166.

(65) S. Sayanagi, "Effect of Hot Rolling Conditions on the Mechanical Properties of Very Low Carbon Ti-Bearing Cold Rolled Steels", Tetsu-To-Hagne, 71 (13) (1985), S1361.

(66) S. Satoh, T. Obara, M. Nishida, and T. Irie, Trans. ISIJ, 24 (1984), 838-846.

(67) H. Katoh, et al., "Cold Rolled Steel Sheets Produced by Continuous Annealing", Technology of Continuously Annealed Cold Rolled Sheet Steel, (TMS-AIME , Warrendale, PA, 1985), 37-60.

(68) W.B. Hutchinson, K.I. Nilsson and J. Hirsch, "Annealing Textures in Ultra-Low Carbon Steels", Metallurgy of Vacuum Degassed Steels, (TMS, Warrendale, PA, 1990), 109-126.

(69) S. Tosaka, "Influence of Hot Rolling Conditions upon Mechanical Properties of ULC Stabilized Steel Sheets for Automobile Use", MWSP, (ISS, Warrendale, PA, 1989), 523-531.

(70) K. Tsuyonama, et at., "Effect of Lowering Sulfur Content in Ti-Added, Deep - Drawable Hot- and Cold- Rolled Sheet Steels", Hot and Cold Rolled Sheet Steels, (TMS, Warrendale, PA, 1988), 155-164.

(71) T. Senuma, Physical Metallurgy for Producing Super Formable Deep Drawing Steel Sheets, Vol. 1, 1988, 157-168.

(72) O. Hashimoto, A. Satoh, T. Irie, N. Ohashi, "Ultra-low C-Nb-P steel sheet with high strength and excellent deep drawability", proc. International Conference on Advances in Physical Metallurgy and Applications of the Steel, (The Metals Society of Great Britain, Book 284, 1982), 95-104.

(73) M.P. Butrón-Guillén and J. J. Jonas, proc. International Forum for Physical Metallurgy of IF Steels, ISIJ, (Tokyo, 1994), 123-126.

(74) W. B. Hutchinson and K. Ushioda, Scand. J. of Metallurgy, 13 (1984), 269.

(75) H. Inagaki, Trans. ISIJ, 24 (1984), 266-274.

(76) M. R. Barnett, J. J. Jonas, and P. D. Hodgson, "A Comparison Between the Recrystallization Behaviors of Warm and Cold Rolled Ferrite" proc. 37th Mechanical Working and Steel Processing Conference, (ISS, Warrendale, PA, 1996, Hamilton, Ontario, Canada).

(77) M. P. Butrón-Guillén and J. J. Jonas, "Effect of Finishing Temperature on Hot Band Textures in an IF Steel", ISIJ, (1996), 68-73.

(78) T. Senuma and H. Yada, proc. Intl. Conf. on Physical Metallurgy of TMP of Steels and other Metals, 2, (The Iron and Steel Institute of Japan, Tokyo, 1998), 636.

(79) T. Nakamura and K. Esaka, proc. Intl. Conf. on Physical Metallurgy of TMP of Steels and other Metals, 2, (The Iron and Steel Institute of Japan, Tokyo, 1998), 644.

(80) L. J. Ruiz-Aparicio, C. I. Garcia, and A J. DeArdo, "The Role of Transformation Textures on the Development of Cold Rolled and Annealing Textures in Ultra-Low Carbon Steels", IF Steels 2000, (ISS, Warrendale, PA, 2000), 85-96.

(81) K. Mahadevan, P. Liang, and J. Fekete, "Effect of Strain Rate in Full Vehicle Frontal Crash Analysis", SAE Paper 00PC-365, (SAE, Warrendale, PA, 2000).

(82) SAE J2329, "Categorization and Properties of Low-Carbon Automotive Sheet Steels", (SAE, Warrendale, PA, 1997).

(83) SAE J2340, "Categorization and Properties of Dent Resistant, High Strength, and Ultra High Strength Automotive Sheet Steel", (SAE, Warrendale, PA, 1999).

(84) JFS A 3011, " Hot-Dip Galvannealed Steel Sheets and Strip for Automobile Use", The Japan Iron and Steel Federation, Japan, 1996.

(85) B. Engl and T. Gerber, "Microalloyed, Vacuum Degassed High-Strength Steels with Special Emphasis on IF Steels", Steel Research, 67 (1996), 430-437.

(86) B. Yan and I. Gupta, " Secondary Work Embrittlement of Interstitial-Free Steels", Modern LC and ULC Sheet Steels for Cold Forming: Processing and Properties, ed. Wolgang Bleck, Verlag Mainz, (Aachen, Germany, 1998), 249-263.

(87) M. Yamada, Y. Tokunaga, and M. Yamamoto, "Effect of Nb and Ti on Resistance to Cold-Work Embrittlement of Extra-Low-Carbon High Strength Cold-Rolled Sheet Containing Phosphorus", Tetsu-to-Hagane, (1987), 1049-1056.

(88) J.S. Rege, M. Hua, C. I. Garcia, A. J. DeArdo, "The Segregation Behavior of Phosphorus in Ti and Ti+Nb Stabilized Interstitial- Free Steels", ISIJ International, 2000, 191-199.

(89) Y. Tokunaga, M. Yamada, andn K. Ito, "Effect of Combined Addition of Nb and Ti on the Mechanical Properties of Extra Low Carbon Steel Sheets", Tetsu-to-Hagane, 73 (1987), 341-348.

(90) D.A. Jones and S.R. Daniel, "A Review of the Development and Use of ULC Steels Manufactured by Corus Group (Wales) and Current Challenges for Further Development", proc. IF Steels 2000, Iron and Steel Society, Warrendale, PA, 2000, pp. 55-68.

(91) Y. Hosoya, T. Urabe, K. Tanikawa, K. Tahara, and A. Nishimoto, "Development of Super-formable High-Strength Interstitial-Free Sheet Steel", Interstitial-Free Steel Sheet: Processing, Fabrication, and Properties, ed. D. L. Baragar, (Canadian Institute of Mining, Metallurgy, and Petroleum, Montreal, 1991), 107-117.

(92) K. Okuda, Y. Kawabata, K. Sakuta, and T. Obara, "Effect of the Hot-Rolling Lunricant Condition in Ferrite Region on the Texture Formation of Cold-Rolled Sheet Steels with Ultra-High r-Value", proc. 39th Mechanical Working and Steel Processing, (Iron and Steel Society, Warrendale, PA, 1998), 297-305.

(93) T. Obara and K. Sakata, "Development of Metallurgical Aspects and Processing Technologies in IF Sheet Steel", proc. 39th Mechanical Working and Steel Processing, (Iron and Steel Society, Warrendale, PA, 1998), 307-314.

(94) K. L. Zeik, E. A. Silva, L. A. Roudabush, E. Gallo, "Effect of Processing Parameters on the Performance of Galvanneal Coatings at U. S. Steel and PRO-TEC Coating Company", (Paper presented at the Galvanizers Association Meeting, October 1993, Baltimore, MD).

(95) A. J. C. Burghardt, A. van der Heiden, E. B. van Perlstein, J. P. Schoen, "Galvanized and Galvannealed IF-Steel of Hoogovens for the Automotive Industry", proc. Galvatech '92, (Amsterdam, 1992), 189-193.

(96) W. Zhong, H. F. Ng, J. M. James, "Correlation Between Adhesion Properties and the Interfacial Bonding Strength of Galvanneal Coatings", Zinc-Based Coating Systems: Production and Performance, ed. F. E. Goodwin, (The Minerals, Metals, and Materials Society, Warrendale, PA, 1998), 185-194.

(97) S. P. Carless, B. D. Jeffs, V. Randle, "Influence of Substrate Topography on the Formation of Iron Zinc Phases and the Properties of Galvanneal Coatings", proc. Galvatech '98, (Chiba, Japan, The Iron and Steel Institute of Japan, 1998), 208-214.

(98) Y. Hisamatsu, "Science and Technology of Zinc and Zinc Alloy Coated Steel Sheet", proc. Galvatech '89, ISIJ, 1989, 3-12.

(99) W. van Koesvald, M. Lamberigts, A. van der Heiden, and L. Bordignon, "Coating Microstructure Assessment and Control for Advanced Product Properties of Galvannealed IF Steels", proc. Galvatech '95, (Iron and Steel Society, Warrendale, PA, 1995), 343-355.

(100) N. Fujibayashi, K. Kyono, C. Kato, N. Morito, "Influence of Carbide-Forming-Elements in Substrate Steels on Galvannealing Behavior", proc. Galvatech '98, (Chiba, Japan, The Iron and Steel Institute of Japan, 1998), 180-184.

(101) E. T. McDevitt, L. Pelayo, Y. Morimoto,and M. Meshii, "Investigation of the Fe-Al Inhibition Layer Formed During Hot-Dip Galvannealing", proc. 39th Mechanical Working and Steel Processing, (Iron and Steel Society, Warrendale, PA 1998), 127-136.

(102) K. Hashiguchi, A. Yasuda, T. Hanazawa, M. Ohri, T. Ichida, "Galvannealed Sheet Steel with Excellent Press Formability", La Revue de Metallurgie, 1990, 277-283.

(103) M. Urai, M. Arimura, and H. Sukai, "Effect of P Content in Ultra Low C-Ti Steel on Galvannealing Behavior", Tetsu-to-Hagane, 80 (1994), 545.

(104) C. S. Lin and M. Meshii, "Effect of Steel Chemistry on the Formation of the Alloy Layers on the Commercial Hot-Dip Coatings", proc. Galvatech '95, (Iron and Steel Society, Warrendale, PA, 1995), 335-342.

(105) I. Hertveldt, B. C. De Cooman, and S. Classens, "Influence of Annealing Conditions on the Galvanizability and Galvannealing Properties of TiNb Interstitial-Free Strengthened with Phosphorus and Manganese", Metall. and Materials Trans. A, 31A (2000), 1225-1232.

(106) C. Kato, "Effect of Si, Mn, and P Addition in Ultra-Low-Carbon Steel Sheets on Hot-Dip Zn Coating Performance", CAMP-ISIJ, 7 (1994), 1511.

(107) C. Coffin and S. W. Thompson, "Galvannealing of Interstitial-Free Sheet Steels Strengthened by Manganese, Silicon, or Phosphorus: an Initial Study", The Physical Metallurgy of Zinc Coated Steel, ed. A. R. Marder, (TMS, Warrendale, PA, 1993), 181-196.